Ueda M, Kawamura N, Tateishi T, Sakae N, Motomura K, Ohyagi Y, Kira JI.	Phenotypic spectrum of hereditary neuralgic amyotrophy caused by the SEPT9 R88W mutation.	*J Neurol Neurosurg Psychiatry.*	81(1)	94-6	2010
Piao H, Minohara M, Kawamura N, Li W, Mizuone Y, Umehara F, Goto Y, Kusunoki S, Matsushita T, Ikenaka K, Maejima T, Nabekura J, Yamasaki R, Kira J	Induction of paranodal myelin detachment and sodium channel loss in vivo by Campylobacter jejuni DNA-binding protein from starved cells (C-Dps) in myelinated nerve fibers.	*J Neurol Sci.*	288(1-2)	54-62	2010
Kirimoto H, Ogata K, Onishi H, Oyama M, Goto Y, Tobimatsu S.	Transcranial direct current stimulation over the motor association cortex induces plastic changes in ipsilateral primary motor and somatosensory cortices.	*Clin Neurophysiol.*	122(4)	777-783	2011
Mitsudo T, Kamio Y, Goto Y, Nakashima T, Tobimatsu S.	Neural responses in the occipital cortex to unrecognizable faces.	*Clin Neurophysiol.*	122(4)	708-718	2011
Hagiwara K, Okamoto T, Shigeto H, Ogata K, Somehara Y, Matsushita T, Kira J, Tobimatsu S.	Oscillatory gamma synchronization binds the primary and secondary somatosensory areas in humans.	*Neuroimage.*	51(1)	412-20	2010
Miyazaki Y, Koike H, Ito M, Atsuta N, Watanabe H, Katsuno M, Kusunoki S, Sobue G.	Acute superficial sensory neuropathy with generalized anhidrosis, anosmia, and ageusia.	*Muscle Nerve.*	43(2)	286-288	2011
Kusunoki S, Kaida K.	Antibodies against ganglioside complexes in Guillain-Barré syndrome and related disorders.	*J Neurochem.*	116(5)	828-832	2011
Saigoh K, Izumikawa T, Koike T, Shimizu J, Kitagawa H, Kusunoki S.	Chondroitin beta-1,4-N-acetylgalactosaminyltransferase-1 missense mutations are associated with neuropathies.	*J Hum Genet.*	56(2)	143--146	2011
Kawagashira Y, Kondo N, Atsuta N, Iijima M, Koike H, Katsuno M, Tanaka F, Kusunoki S, Sobue G	IgM MGUS anti-MAG neuropathy with predominant muscle weakness and extensive muscle atrophy.	*Muscle Nerve.*	42(3)	433--435	2010
Ueda A, Shima S, Miyashita T, Ito S, Ueda M, Kusunoki S, Asakura K, Mutoh T.	Anti-GM1 antibodies affect the integrity of lipid rafts.	*Mol Cell Neurosci.*	45(4)	355-362	2010
Tomita M, Watanabe H, Morozumi S, Kawagashira Y, Iijima M, Nakamura T, Katsuno M, Koike H, Hattori N, Hirayama M, Kusunoki S, Sobue G.	Pyramidal tract involvement in Guillain-Barré syndrome associated with anti-GM1 antibody.	*J Neurol Neurosurg Psychiatry.*	81(5)	583-585	2010
Kaida K, Kusunoki S.	Antibodies to gangliosides and ganglioside complexes in Guillain-Barré syndrome and Fisher syndrome: mini-review.	*J Neuroimmunol.*	223(1-2)	5-12	2010

Curb JD, Ueshima H, Rodriguez BL, He Q, Koropatnick TA, Nakagawa H, Sakata K, Saitoh S, Okayama A	Differences in lipoprotein particle subclass distribution for Japanese Americans in Hawaii and Japanese in Japan: the INTERLIPID study.	*J Clin Lipidol.*	5(1)	30-36	2011
Yokokawa H, Yasumura S, Tanno K, Ohsawa M, Onoda T, Itai K, Sakata K, Kawamura K, Tanaka F, Yoshida Y, Nakamura M, Terayama Y, Ogawa A, Okaya	Serum low-density lipoprotein to high-density lipoprotein ratio as a predictor of future acute myocardial infarction among men in a 2.7-year cohort study of a Japanese northern rural population.	*J Atheroscler Thromb.*	18(2)	89-98	2011
Suwazono Y, Nogawa K, Uetani M, Miura K, Sakata K, Okayama A, Ueshima H, Stamler J, Nakagawa H.	Application of hybrid approach for estimating the benchmark dose of urinary cadmium for adverse renal effects in the general population of Japan.	*J Appl Toxicol.*	31(1)	89-93	2011
Tanno K, Okamura T, Ohsawa M, Onoda T, Itai K, Sakata K, Nakamura M, Ogawa A, Kawamura K, Okayama A.	Comparison of low-density lipoprotein cholesterol concentrations measured by a direct homogeneous assay and by the Friedewald formula in a large community population.	*Clin Chim Acta.*	411(21-22)	1774-1780	2010
Guo Z, Miura K, Turin TC, Hozawa A, Okuda N, Okamura T, Saitoh S, Sakata K, Nakagawa H, Okayama A, Yoshita K, Kadowaki T, R Choudhury S, Nakamura Y, L Rodriguez B, Curb JD, Elliott P, Stamler J, Ueshima H.	Relationship of the Polyunsaturated to Saturated Fatty Acid Ratio to Cardiovascular Risk Factors and Metabolic Syndrome in Japanese: the INTERLIPID Study.	*J Atheroscler Thromb.*	17(8)	777-784	2010
Ohsawa M, Kato K, Itai K, Tanno K, Fujishima Y, Konda R, Okayama A, Abe K, Suzuki K, Nakamura M, Onoda T, Kawamura K, Sakata K, Akiba T, Fujioka	Standardized prevalence ratios for chronic hepatitis C virus infection among adult Japanese hemodialysis patients.	*J Epidemiol.*	20(1)	30-9	2010
Mizutamari M, Sei A, Tokiyoshi A, Fujimoto T, Taniwaki T, Togami W, Mizuta H.	Corresponding scapular pain with the nerve root involved in cervical radiculopathy.	*J Orthop Surg (Hong Kong).*			in press
Miura S, Shibata H, Kida H, Noda K, Toyama T, Iwasaki N, Iwaki A, Ayabe M, Aizawa H, Taniwaki T, Fukumaki Y.	Partial SPAST and DPY30 deletions in a Japanese spastic paraplegia type 4 family.	*Neurogenetics.*	12(1)	25-31	2011
Miura S, Azuma K, Yamada K, Takamori S, Kawahara A, Noda K, Ayabe M, Kage M, Aizawa H, Taniwaki	Combined treatment with prednisolone and tacrolimus for myasthenia gravis with invasive thymoma.	*Acta Neurol Belg.*	110(1)	107-109	2010

Miyake Y, Sasaki S, Tanaka K, Fukushima W, Kiyohara C, Tsuboi Y, Yamada T, Oeda T, Miki T, Kawamura N, Sakae N, Fukuyama H, Hirota Y, Nagai M.	Dietary fat intake and risk of Parkinson's disease: a case-control study in Japan.	*J Neurol Sci.*	288(1-2)	117-122	2010
Murakami K, Miyake Y, Sasaki S, Tanaka K, Fukushima W, Kiyohara C, Tsuboi Y, Yamada T, Oeda T, Miki T, Kawamura N, Sakae N, Fukuyama H, Hirota Y, Nagai M.	Dietary glycemic index is inversely associated with the risk of Parkinson's disease: a case-control study in Japan.	*Nutrition.*	26(5)	515-521	2010

研究成果の刊行物（別刷）

Brain Pathology ISSN 1015-6305

RESEARCH ARTICLE

Reappraisal of Aquaporin-4 Astrocytopathy in Asian Neuromyelitis Optica and Multiple Sclerosis Patients

Takeshi Matsuoka[1,2]; Satoshi O. Suzuki[2]; Toshihiko Suenaga[3]; Toru Iwaki[2]; Jun-ichi Kira[1]

[1] Departments of Neurology and [2] Neuropathology, Neurological Institute, Graduate School of Medical Sciences, Kyushu University, Fukuoka, Japan.
[3] Department of Neurology, Tenri Hospital, Tenri, Japan.

Keywords
antibody, aquaporin-4, astrocyte, multiple sclerosis, neuromyelitis optica.

Corresponding author:
Satoshi O. Suzuki, MD, PhD, Department of Neuropathology, Neurological Institute, Graduate School of Medical Sciences, Kyushu University, 3-1-1 Maidashi, Higashi-ku, Fukuoka 812-8582, Japan (E-mail: *sosuzuki@np.med.kyushu-u.ac.jp*)

Received 11 August 2010; accepted 9 December 2010.

doi:10.1111/j.1750-3639.2011.00475.x

Abstract

Selective aquaporin-4 (AQP4) loss and vasculocentric complement and immunoglobulin deposition are characteristic of neuromyelitis optica (NMO). We recently reported extensive AQP4 loss in demyelinated and myelinated layers of Baló's lesions without perivascular immunoglobulin and complement deposition. We aimed to reappraise AQP4 expression patterns in NMO and multiple sclerosis (MS). We evaluated AQP4 expression relative to glial fibrillary acidic protein, extent of demyelination, lesion staging (CD68 staining for macrophages), and perivascular deposition of complement and immunoglobulin in 11 cases with NMO and NMO spectrum disorders (NMOSD), five with MS and 30 with other neurological diseases. The lesions were classified as actively demyelinating (n = 66), chronic active (n = 86), chronic inactive (n = 48) and unclassified (n = 12). Six NMO/NMOSD and two MS cases showed preferential AQP4 loss beyond the demyelinated areas, irrespective of lesion staging. Five NMO and three MS cases showed AQP4 preservation even in actively demyelinating lesions, despite grave tissue destruction. Vasculocentric deposition of complement and immunoglobulin was detected only in NMO/NMOSD patients, with less than 30% of actively demyelinating lesions showing AQP4 loss. Our present and previous findings suggest that antibody-independent AQP4 loss can occur in heterogeneous demyelinating conditions, including NMO, Baló's disease and MS.

Abbreviations: ALS = amyotrophic lateral sclerosis; AQP4 = aquaporin-4; BBB = blood-brain barrier; BCS = Baló's concentric sclerosis; CNS = central nervous system; GFAP = glial fibrillary acidic protein; H & E = hematoxylin and eosin, IgG = immunoglobulin G; KB = Klüver-Barrera; LESCL = longitudinally extensive spinal cord lesion; MG = myasthenia gravis; MS = multiple sclerosis; MRI = magnetic resonance imaging; NMO = neuromyelitis optica; NMOSD = neuromyelitis optica spectrum disorder; OSMS = opticospinal multiple sclerosis; SCD = spinocerebellar degeneration; SPG = spastic paraplegia.

INTRODUCTION

Multiple sclerosis (MS) and neuromyelitis optica (NMO) are inflammatory demyelinating diseases of the central nervous system (CNS). The pathological hallmark in MS is sharply demarcated demyelinating plaques with axons relatively preserved, suggesting autoimmune attacks targeting CNS myelin. By contrast, NMO shows selective and severe attacks on both axons and myelin of the optic nerves and spinal cord, resulting in necrotic cavitation. In this condition, longitudinally extensive spinal cord lesions (LESCLs) extending over three vertebral segments are characteristic on magnetic resonance imaging (MRI) (54).

Although the nosological position of NMO has long been a matter of debate, the recent discovery of a specific IgG against NMO, designated NMO-IgG (28), suggests that NMO is distinct from MS and has a fundamentally different etiology. This IgG targets the aquaporin-4 (AQP4) water channel protein (29), which is strongly expressed on astrocyte foot processes at the blood–brain barrier (BBB) (18). Autopsied NMO cases show a loss of AQP4 immunostaining in inflammatory lesions (38, 45). The vasculocentric deposition of complement and immunoglobulins in NMO lesions (30) suggests a humoral immune attack against AQP4 on astrocytes, especially as the NMO-IgG/anti-AQP4 antibody is cytotoxic to astrocytes *in vitro* and *in vivo* in the presence of complement (3, 5, 19–21, 46, 47, 52).

However, the predictive value of the NMO-IgG/anti-AQP4 antibody is only moderate; 30%–73% in Caucasians (9, 10, 17, 28, 42), 63% in northern Japanese with opticospinal MS (OSMS) (39), 27% in southern Japanese with OSMS (31) and 33% in Caribbean people (6). On the other hand, 5%–15% of MS cases are positive for NMO-IgG or anti-AQP4 antibody. Pittock *et al* (43) described that 10% of NMO-IgG-positive patients had brain lesions that were

Table 1. Summary of clinical and pathological findings of Japanese patients with neuromyelitis optica and multiple sclerosis. Abbreviations: MS = multiple sclerosis; N.A. = not applicable; NMO = neuromyelitis optica (Wingerchuk *et al* (55, 56)); NMOSD = neuromyelitis optica spectrum disorders (Wingerchuk *et al* (57)).

Autopsy	Age (years)	Sex	Disease duration (years)	Relapse rate	Clinically estimated sites of lesions	Pathologically determined sites of lesions
NMO-1	44	F	3.8	1.6	O2, S6	O, S, Bs, Cr, Cl
NMO-2	44	F	1.8	2.8	O2, Bs3, S2	O, S, Bs, Cr
NMO-3	48	F	0.5	4.0	O2, Bs1, S1	O, S, Bs, Cr
NMO-4	32	M	6.3	1.1	O1, Bs2, S7	O, S, Bs, Cl, Cr
NMO-5	28	F	4.7	0.6	O3, Bs2, S2	O, S, Bs, Cl, Cr
NMO-6	35	F	7.0	1.4	O4, Bs4, S4	O, S, Bs, Cr
NMO-7	37	F	10.8	1.5	O9, Bs2, S14	O, S, Bs, Cl, Cr
NMO-8	47	F	8.3	0.1	O2, Bs1, S2	O, S, Bs, Cr
NMO-9	54	F	4.0	1.3	O1, S6	O, S
NMO-10*	37	F	17.0	1.1	O8, Bs1, S9, Cr3	Bs, S, Cr
NMOSD	88	M	0.4	0.0	S1	O, S
MS-1	12	F	5.0	2.2	O6, Bs1, S2, Cr3	O, Bs, S, Cr, Cl
MS-2	35	M	3.1	1.0	O1, Bs2, S2, Cr2	O, Bs, S, Cr
MS-3	52	F	1.3	1.5	Bs1, Cr3	Bs, Cr
MS-4	45	F	0.7	1.4	Bs2, S2	O, S, Bs
MS-5	39	M	21.0	0.5	O1, Bsx, Clx, Crx	O, Bs, Cl, Cr

Lesion sites in clinical exacerbations: O = optic nerve; S = spinal cord; Bs = brainstem; Cl = cerebellum; Cr = cerebrum. Numbers indicate exacerbations in each lesion site (eg, O2 represents two episodes of optic neuritis). Asterisk indicates a NMO case with known anti-AQP4 antibody seropositivity.

indistinguishable from those in MS patients, whereas some patients also showed extensive brain lesions (34, 36, 43). By contrast, LESCLs are seen in about a quarter of classical Asian MS patients (8, 32, 37, 49), compared with 12.5% of Caucasian MS patients (4). Asian patients with MS show necrotizing lesions with occasional cavity formation in the spinal cord, optic nerve and cerebrum (12, 14, 40, 50), reflecting severe inflammation. These findings suggest considerable overlap between NMO and MS, especially in Asians.

In addition, Baló's concentric sclerosis (BCS), a rare variant of MS with huge brain lesions showing concentric rings of alternating demyelination and normal myelin layers, is more common in Asians, such as Filipinos (25), southern Han Chinese (53) and Taiwanese (7), than in other races. Asian MS patients can also show concentric demyelinating lesions in the spinal cord and the optic chiasm pathologically (16), representing an intermediate between BCS and MS. We recently reported extensive AQP4 loss in both demyelinated and myelinated layers of BCS lesions in the absence of perivascular immunoglobulin and complement deposition (33). Interestingly, development of BCS-like lesions in the brainstem on MRI was recently reported in Asian patients with not only classical MS (23) but also NMO (11). Other than two pivotal neuropathological studies (38, 45), only a few case reports have examined AQP4 expression in NMOs with varying results (13, 24, 51, 57). Furthermore, although AQP4 expression in MS has also been examined in some studies (38, 45, 48), there are inconsistencies

Table 2. Antibodies used for immunohistochemistry. Abbreviations: AQP4 = aquaporin-4; GFAP = glial fibrillary acidic protein; N.D. = not done.

Antibody	Type	Dilution	Antigen retrieval	Source
Aquaporin-4				
AQP4	rabbit polyclonal	1:500	N.D.	Santa Cruz Biotechnology, California, USA
Complement				
C3d	rabbit polyclonal	1:1000	Autoclave/10 mM citrate buffer	DakoCytomation, Glostrup, Denmark
C9neo	mouse monoclonal	1:1000	Autoclave/10 mM citrate buffer	Abcam plc, Cambridge, UK
Macrophage/microglia				
CD68	mouse monoclonal	1:200	Autoclave/10 mM citrate buffer	DakoCytomation, Glostrup, Denmark
Astrocyte				
GFAP	rabbit polyclonal	1:1000	N.D.	DakoCytomation, Glostrup, Denmark
Immunoglobulin				
IgG	rabbit polyclonal	1:10 000	Autoclave/10 mM citrate buffer	DakoCytomation, Glostrup, Denmark
IgM	rabbit polyclonal	1:10 000	Autoclave/10 mM citrate buffer	DakoCytomation, Glostrup, Denmark
Lymphocyte				
CD45RO	mouse monoclonal	1:200	Autoclave/10 mM citrate buffer	DakoCytomation, Glostrup, Denmark
CD20	mouse monoclonal	1:200	Autoclave/10 mM citrate buffer	DakoCytomation, Glostrup, Denmark

Table 3. Classification of demyelinating lesions according to aquaporin-4 and glial fibrillary acid protein immunostaining and Klüver-Barrera staining. Abbreviations: AQP4 = aquaporin-4; GFAP = glial fibrillary acidic protein; KB = Klüver-Barrera staining.

Lesion pattern	Extents of AQP4 and myelin loss	GFAP expression
Pattern A	AQP4 loss or decrease > myelin loss	(+)
Pattern B	AQP4 loss or decrease = myelin loss	(+)
Pattern C	AQP4 loss or decrease < myelin loss	(+)
Pattern D	AQP4 totally preserved in areas of myelin loss	(+)
Pattern N	necrosis or cavity formation	(–)

among their conclusions. We therefore decided to perform a systematic immunohistological reappraisal of AQP4 expression relative to astrocyte marker expression, the extent of demyelination, lesion staging and the perivascular deposition of complement and immunoglobulin in Asian NMO and MS patients to clarify the contribution of astrocyte damage, including AQP4 loss to the lesion formation, in these conditions.

MATERIALS AND METHODS

Autopsy tissue and patient characterization

The study was performed on archival autopsied brain, optic nerve and spinal cord materials from 10 NMO cases, including one anti-AQP4 antibody-positive case, one case with NMO spectrum disorder (NMOSD), and five cases with MS. All but the anti-AQP4 antibody-positive case from Tenri Hospital were from the Department of Neuropathology, Kyushu University. NMO/NMOSD diagnosis was based on the Wingerchuk criteria (54–56), while MS was diagnosed according to the Poser criteria (44). The clinical findings are summarized in Table 1. The median age at autopsy was 44.0 years old (range 28–88) in the NMO/NMOSD cases (nine females and two males) and 39.0 years old (range 12–52) in the MS cases (three females and two males). Disease durations ranged from 0.4

Table 4. Summary of aquaporin-4 immunoreactivity patterns in demyelinating lesions in cases with neuromyelitis optica (NMO) or NMO spectrum disorders. Abbreviations: AQP4 = aquaporin-4; NMO = neuromyelitis optica; NMOSD = neuromyelitis optica spectrum disorder; N.A. = specimen not available.

Autopsy	Stage	Cerebrum	Brainstem	Cerebellum	Spinal cord	Optic nerve
Preferential AQP4 loss or decrease						
NMO-2	Active	A (1)	A&N (1)	N.A.	B&N (1)	N.A.
	Chronic active	B&N (1), C&N (1)			A&N (3), B&N (1)	
	Chronic inactive	C (2)			C&N (1)	
NMO-3	Active	B&N (1)				A&N (1)
	Chronic active	B&N (1), C&N (1)	A (1)		A&N (3)	A&N (1)
	Chronic inactive	C&N (3)				
NMO-4	Active	A (1), A&N (3), B (1), B&N (1)	A&N (2), B&N (1)	B (2)	B&N (1)	D (1)
	Chronic active	B&N (1)	B (2)		A&N (1), B&N (1), C&N (1)	
	Chronic inactive	D (1)				
NMO-7	Active		A (3), B (1)		A&N (2)	
	Chronic active	C (3)	A (3), B (1), C (1), C&N (1)			
	Chronic inactive	C (1), D (2)	C&N (2)			D&N (1)
NMO-10	Active	A (1), A&N (1), N (1)				N.A.
	Chronic active	B (2), B&N (1), C&N (1)	C&N (1)		A&N (1), C&N (1)	
	Chronic inactive	D (1), N (1)				
NMOSD	Active				A&N (1), B&N (1), N (1)	
	Chronic active				B&N (1)	
	Chronic inactive					D (1)
Preserved AQP4 expression						
NMO-1	Active	D&N (1)	N (2)			
	Chronic active		D (1)		D (1)	D (1)
	Chronic inactive	D&N (1)				
NMO-5	Active	D&N (1), D (3)				
	Chronic active	D (5), D&N (4)	D&N (1), D (2)	D (2)		
	Chronic inactive	D (3)	D&N (1)		D&N (1)	D (1)
NMO-6	Active	D (1)				
	Chronic active	D (5), D&N (2)	D&N (1)	D (1)		
	Chronic inactive	D (1)	D&N (1)		D (1), D&N (1)	D&N (1)
NMO-8	Chronic active	D (1), D&N (5)	D&N (1)		D&N (1)	D (1)
	Chronic inactive	D (1), D&N (1)	D (2), N (1)			N (1)
NMO-9	Active				D&N (1), N (2)	D (1)
	Chronic active				D&N (1)	

Blank cell = No lesions.

to 17.0 years in the NMO/NMOSD group (median, 4.7 years), and from 0.7 to 21.0 years in the MS group (median, 3.1 years). In addition, we used the same set of control cases with other neurological diseases as in our previous study (33): myasthenia gravis (MG) (n = 2), spastic paraplegia type 2 (n = 1), amyotrophic lateral sclerosis (n = 6), hippocampal sclerosis with temporal lobe epilepsy (n = 5), muscular dystrophy (n = 1), encephalitis (n = 3), including one with anti-N-methyl-D-aspartate receptor antibody and another with anti-thyroglobulin antibody, spinocerebellar degeneration (n = 1), vasculitis (n = 3), cerebral infarction (n = 1), Pick's disease (n = 1), progressive supranuclear palsy (n = 3) and multiple system atrophy (n = 3).

Tissue preparation and immunohistochemistry

Autopsied specimens were fixed in 10% formalin and processed into paraffin sections. Sections were routinely stained with hematoxylin and eosin (H & E), Klüver-Barrera (KB), and Bodian or Bielschowsky silver impregnation. Primary antibodies for immunohistochemistry are listed in Table 2. All sections were deparaffinized in xylene and rehydrated in an ethanol gradient. Endogenous peroxidase activity was blocked with 0.3% H_2O_2/methanol. The sections were then incubated with primary antibody at 4°C overnight. After rinsing, the sections were subjected to either a streptavidin-biotin complex method or an enhanced indirect immunoperoxidase method using Envision (DakoCytomation, Glostrup, Denmark). Immunoreactivity was detected using 3,3′-diaminobenzidine and sections were counterstained with hematoxylin. Immunohistochemistry for activated complement, immunoglobulins, T cell and B cell markers was performed in randomly selected lesions.

Staging of demyelinating lesions

We classified demyelinating lesions into the following three stages: actively demyelinating lesions, chronic active lesions and chronic inactive lesions based on the density of infiltrating macrophages (26). Briefly, actively demyelinating lesions had active destructive lesions densely and diffusely infiltrated with macrophages phagocytosing myelin debris, as identified by Luxol fast blue staining. Chronic active lesions were those showing hypercellularity of macrophages restricted to the periphery of the lesions. Chronic inactive lesions were those showing no increase in macrophages throughout the lesions.

According to the staging protocol, NMO lesions (n = 149) were classified as 42 actively demyelinating lesions, 72 chronic active lesions and 35 chronic inactive lesions, whereas MS lesions (n = 51) were classified into 24 actively demyelinating lesions, 14 chronic active lesions and 13 chronic inactive lesions. In addition, we noted 12 lesions in NMO (seven lesions) and MS cases (five lesions) that did not meet the staging criteria. All of these lesions had perivascular deposition of both activated complement and immunoglobulins, but no macrophage infiltration, and lacked any myelin or AQP4 loss. These lesions were thus analyzed separately.

Comparison of AQP4 expression with myelin loss and astrogliosis

For each lesion, we compared the level of AQP4 expression with the degree of myelin loss and the level of glial fibrillary acidic protein (GFAP) expression. AQP4 expression levels in region-matched unaffected areas (ie, gray matter or white matter) in the same section were used as an internal control. When the presence of astrocytes was not confirmed by GFAP immunostaining caused by total replacement of a lesion with foamy macrophages, or when cavity formation was evident, the lesion was classified as a destructive necrotic lesion. Accordingly, 15 lesions with severe necrosis or cavity formation (nine in NMO patients and six in MS patients) were determined.

Using serial sections of demyelinating lesions, we divided the expression patterns of AQP4 immunoreactivity relative to the intensity of GFAP immunoreactivity and myelin (KB) staining into the following five patterns (Table 3): Pattern A (area of diminished AQP4 immunoreactivity extending over that of myelin loss), Pattern B (area of diminished AQP4 immunoreactivity conforming with that of myelin loss), Pattern C (area of diminished AQP4 immunoreactivity less than that of myelin loss), Pattern D (preserved AQP4 immunoreactivity with loss of myelin staining) and Pattern N (necrosis or cavity formation; GFAP-negative, AQP4-negative and myelin-negative by definition). Patterns associated with focal necrosis or cavity formation were expressed as "Patterns X & N" (X = A, B, C or D).

Figure 1. Loss of AQP4 expression in active lesions of NMO. **(A–F)** Serial sections of an actively demyelinating cerebral lesion from NMO-10 with known anti-AQP4 antibody seropositivity representing Pattern A. Arrowheads indicate the same blood vessel. **A.** Sharply demarcated demyelinating plaque is noted in the cerebral white matter. **B.** GFAP immunopositivity is decreased in the lesion. **C.** AQP4 immunopositivity is lost beyond the area with myelin/GFAP loss. **D.** Numerous macrophages contain myelin debris (arrowheads). **E.** Degeneration of vascular foot processes is evident by GFAP immunostaining. **F.** AQP4 immunoreactivity is absent even in the degenerated astrocytes. **(G–O)** Serial sections of corpus callosum lesions from NMO-4 representing Patterns A & N. **G.** The corpus callosum demonstrates severe demyelination with tissue necrosis (dagger). **H.** CD68-positive macrophages diffusely infiltrate the lesions. **I.** GFAP immunostaining shows numerous reactive astrocytes in the surrounding region, but it decreases in the necrotic lesion center and focal perivascular areas with positive myelin staining (arrowhead in G and I). **J.** AQP4 immunostaining reveals a pattern similar to that of GFAP staining, but decreases more extensively in the still-myelinated area indicated by the asterisk in G. **K.** High magnification of the necrotic area indicated by the dagger in G. Numerous foamy macrophages containing myelin debris are present. (L–O) High magnification of the still-myelinated area indicated by the asterisk in G. **L.** Still-preserved myelin with some foamy macrophages without myelin debris. **M.** CD68-immunopositive foamy macrophages are present among the preserved myelin. **N.** GFAP immunostaining reveals degenerated astrocytes and astrocytic vascular foot processes. **O.** AQP4 immunoreactivity is completely lost despite the presence of astrocytes. **A, D, G, K, L, KB; B, E, I, N**, GFAP immunohistochemistry (IHC); **C, F, J, O**, AQP4 IHC; H, M, CD68 IHC. Scale bar = 1 mm **(A–C)**; 300 μm **(G–J)**; 50 μm **(E, F, L–O)**; 20 μm **(D, K)**. AQP4 = aquaporin-4; GFAP = glial fibrillary acidic protein; KB = Klüver-Barrera staining; NMO = neuromyelitis optica.

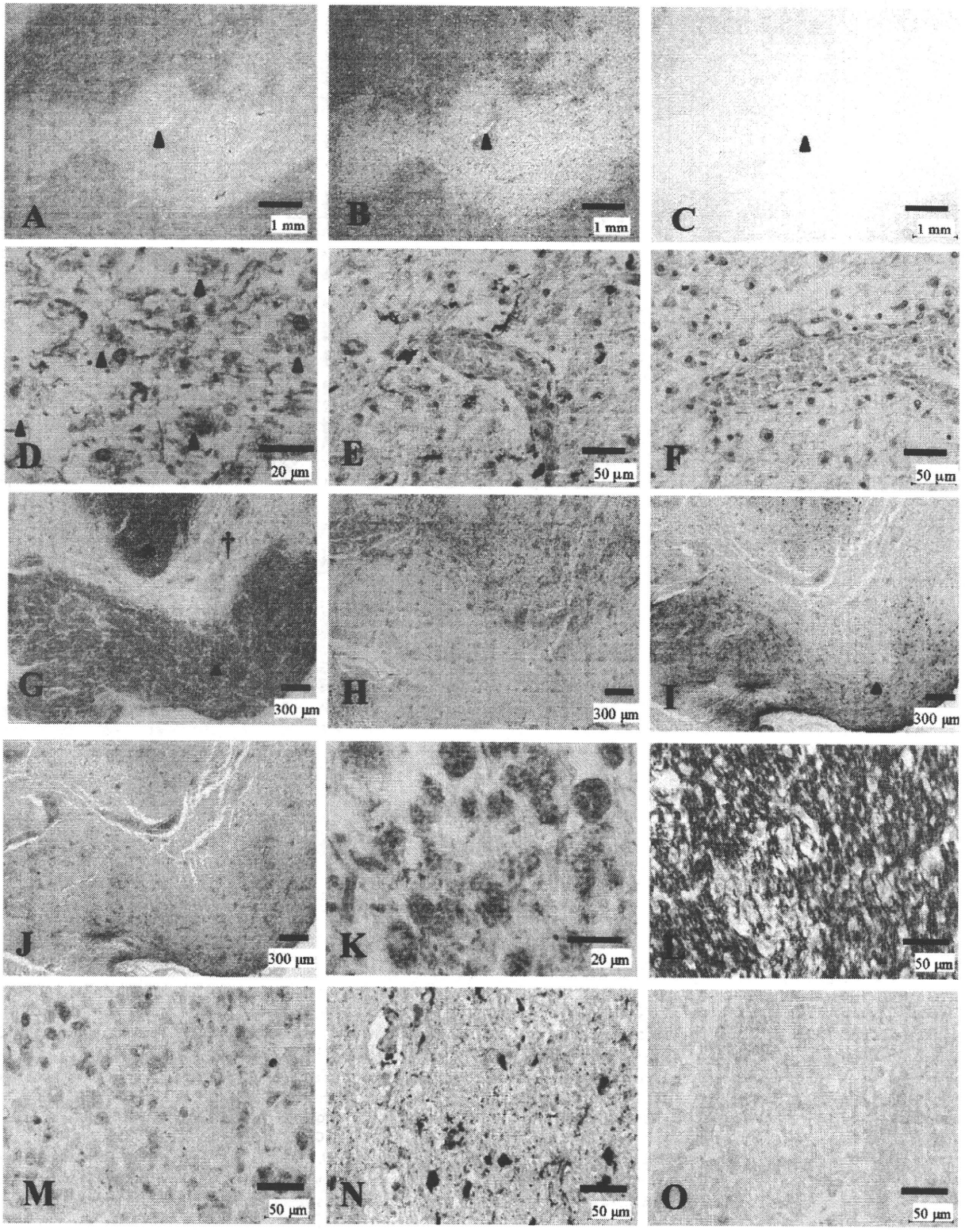

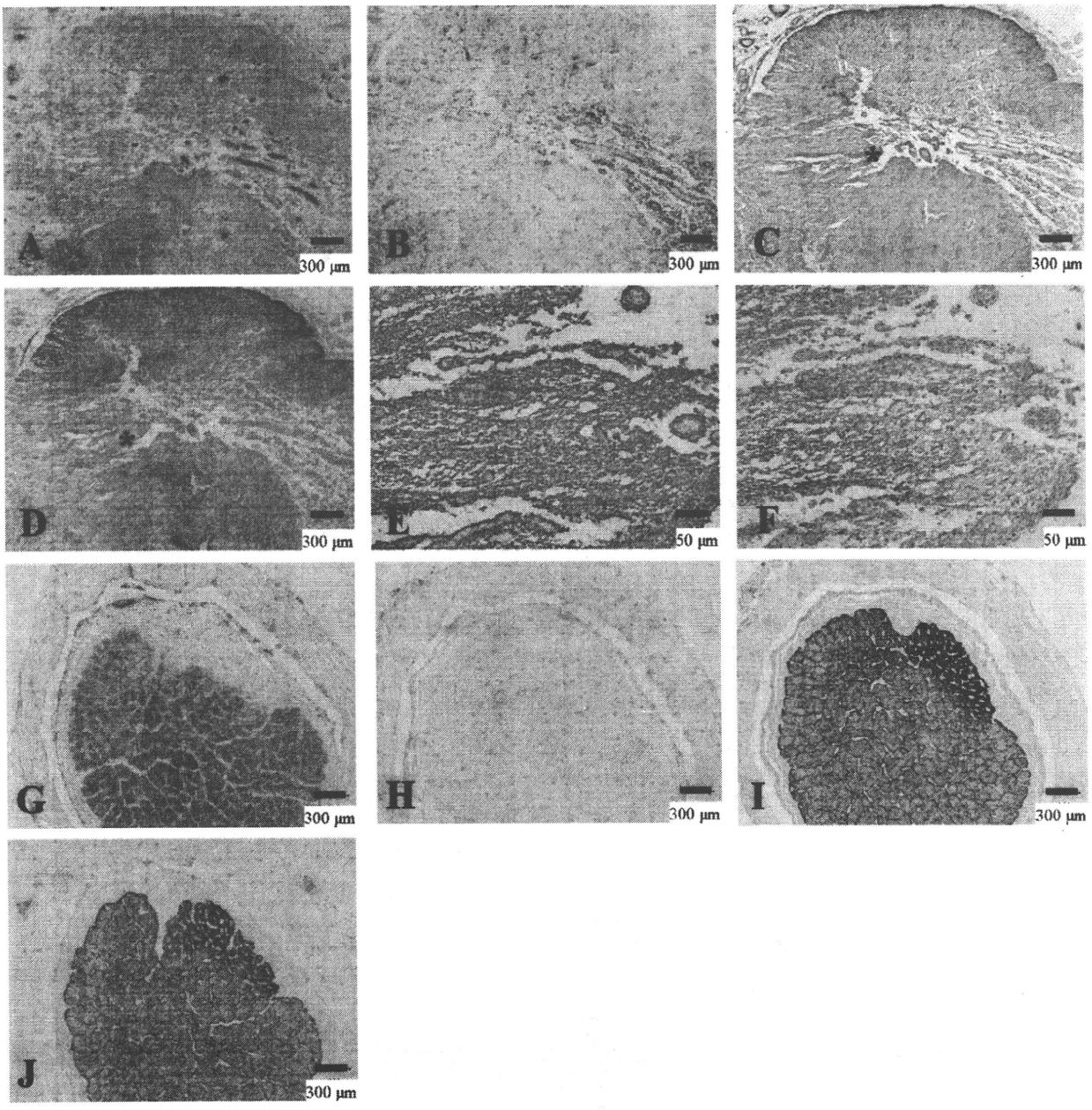

Figure 2. Upregulation of AQP4 in chronic NMO lesions. (**A–F**) Serial sections of chronic active demyelinating lesions in the spinal cord of NMO-10 representing Pattern C and N. **A.** The spinal cord has irregularly-shaped demyelinating lesions with necrosis and cavity formation. Reactive proliferation of capillary vessels is noted. **B.** CD68-positive macrophages are still abundant in the perivascular regions. **C.** The lesion is immunopositive for GFAP except for in the cavity center. **D.** Upregulation of AQP4 in extensively demyelinated lesions. **E.** High magnification in the lesion indicated by the asterisk in C shows increased GFAP immunoreactivity. **F.** The same area as E demonstrates AQP4 staining in areas of astrogliosis. (**G–J**) Serial sections of chronic inactive demyelinating lesions in the optic nerve from NMOSD, representing Pattern D. **G.** Sharply demarcated demyelinating plaque in the optic nerve. **H.** Macrophage infiltration is absent. **I.** GFAP-positive chronic astrogliosis covers the demyelinating plaque. **J.** AQP4 expression is upregulated in the areas of chronic astrogliosis. **A, G**, KB staining; **B, H**, CD68 immunohistochemistry (IHC); **C, E, I**, GFAP IHC; **D, F, J**, AQP4 IHC. Scale bar = 300 μm (**A–D, G–J**); 50 μm (**E, F**). AQP4 = aquaporin-4; GFAP = glial fibrillary acidic protein; KB = Klüver-Barrera staining; NMO = neuromyelitis optica; NMOSD = NMO spectrum disorder.

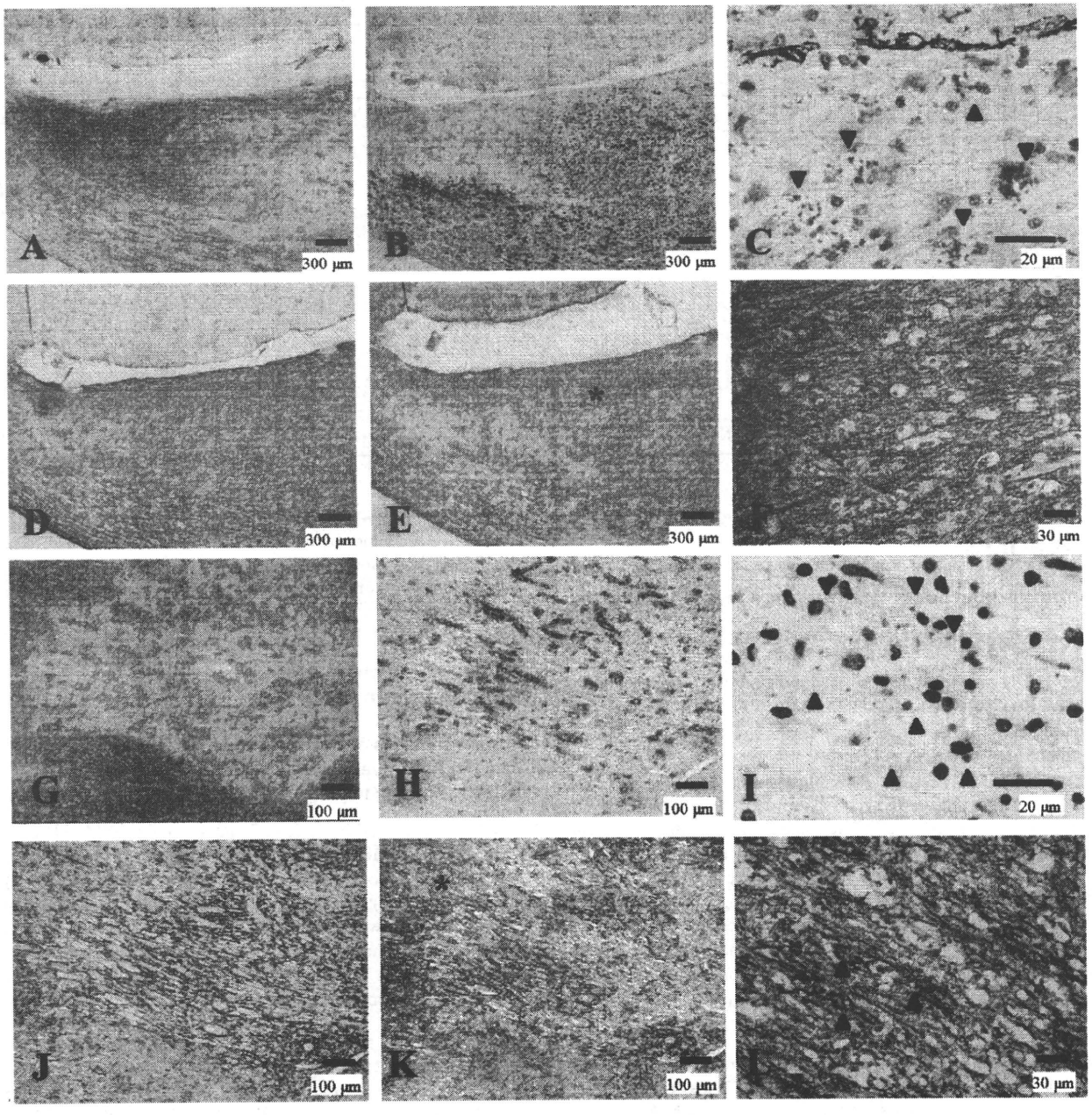

Figure 3. Preserved AQP4 immunoreactivity in actively demyelinating NMO lesions. (**A–F**) Serial sections of an actively demyelinating lesion from NMO-6 representing Pattern D. **A.** Demyelinating plaque in the corpus callosum. **B.** The lesion is infiltrated by numerous foamy macrophages stained with CD68. **C.** Macrophages containing myelin debris (arrowheads). **D.** The lesion shows strong GFAP immunoreactivity. **E.** The same area as in **D**, with AQP4 expression as strong and diffuse as that of GFAP. **F.** High magnification of the area indicated by the asterisk in **E.** AQP4 expression is preserved despite dense macrophage infiltration. (**G–L**) Serial sections of an optic nerve lesion from NMO-4 representing Pattern D. **G.** Sharply demarcated demyelinating plaques are seen. **H.** The optic chiasm is densely infiltrated with foamy macrophages. **I.** Numerous macrophages contain myelin debris. **J.** Numerous GFAP-positive reactive astrocytes in the lesion center and the surrounding areas. **K.** AQP4 immunoreactivity is enhanced at the lesion center. **L.** High magnification of the area indicated by the asterisk in **K** demonstrates AQP4 staining along the entire processes and outlining the cytoplasm of hypertrophic reactive astrocytes (arrowheads). **A, C, G, I**, KB staining; **B, H**, CD68 immunohistochemistry (IHC); **D, J**, GFAP IHC; **E, F, K, L**, AQP4 IHC. Scale bar = 300 μm (**A, B, D, E**); 100 μm (**G, H, J, K**);30 μm (**F, L**); 20 μm (**C, I**). AQP4 = aquaporin-4; GFAP = glial fibrillary acidic protein; KB = Klüver-Barrera staining; NMO = neuromyelitis optica.

Table 5. Summary of aquaporin-4 immunoreactivity patterns in demyelinating lesions in cases with multiple sclerosis. Abbreviations: AQP4 = aquaporin-4; MS = multiple sclerosis.

Autopsy	Stage	Cerebrum	Brainstem	Cerebellum	Spinal cord	Optic nerve
Preferential AQP4 loss or decrease						
MS-3	Active	A&N (1), B (3), B&N (1), N (1)	A&N (2), N (2)			
	Chronic active	B (2)				
	Chronic inactive	C (1)				
MS-4	Active		A (1), B (3)			
	Chronic active		B (1)		A &N (3), A (1)	C (1)
Preserved AQP4 expression						
MS-1	Active		N (3)			
	Chronic active	D&N (1)				
	Chronic inactive				D (1), D&N (2)	
MS-2	Active		D (1), D&N (1)			D (1)
	Chronic active		D (2)			D (1)
MS-5	Active	D (2)	D (1)	D (1)		
	Chronic active	D (1)	D (1)			
	Chronic inactive	D (4), D&N (3)		D (1)		D (1)

Blank cell = no lesions.

RESULTS

Immunohistochemical findings in control brains

AQP4 and GFAP staining patterns as well as the deposition of immunoglobulins and activated complement in normal and diseased CNS tissues were described in detail in our previous report (33). Briefly, in normal cerebral tissues, AQP4 staining was more pronounced in the cortex than in the white matter, with staining emphasized in the perivascular foot processes. The glial limiting membranes and subependymal astrocytes also strongly expressed AQP4. By contrast, GFAP immunoreactivity was preferentially observed in the cerebral white matter while in the cortex, and except for the strong staining of the glial limiting membranes, only a few astrocytes were immunopositive for GFAP. Reactive astrocytes and gliotic scars were strongly immunopositive for both AQP4 and GFAP. In control cases, faint, diffuse IgG immunoreactivity in the neuronal soma, neuropil, oligodendrocytes, astrocytes, glial limiting membranes and ependymal epithelium was observed, but not in the white matter. IgM, C3d and C9neo immunoreactivities were generally confined to a small number of blood vessel walls and the perivascular regions, if any. Activated complement was not usually co-localized with immunoglobulins.

Immunohistochemical findings in NMO and NMO spectrum disorders

Preferential loss or decrease of AQP4 immunoreactivity in actively demyelinating lesions and upregulation of AQP4 in chronic inactive lesions in NMO/NMOSD cases

Five NMO cases (NMO-2, 3, 4, 7 and 10) and an NMOSD case showed preferential loss of AQP4 in at least one of the actively demyelinating lesions beyond the demyelinated areas (Pattern A) (Figure 1, Table 4). NMO-10, with known anti-AQP4 antibody seropositivity, showed extensive AQP4 loss, not only in the lesion center where numerous myelin-laden foamy macrophages had infiltrated (Figure 1D), but also in the surrounding, GFAP-immunopositive myelinated areas (Figure 1A–C). In actively

Figure 4. Preferential loss of AQP4 immunoreactivity in MS. (**A–F**) Serial sections of actively demyelinating lesions in the midbrain of MS-3 without optic-spinal lesions representing Patterns A & N. **A.** A demyelinating plaque in the acute stage in the cerebral peduncle, with dense perivascular lymphocytic cuffing. Myelin is still preserved at the periphery of the lesion (asterisk) despite CD68-positive foamy macrophage infiltration (**B**). **C.** GFAP immunoreactivity is decreased in the lesion center while numerous reactive astrocytes are present at the lesion edge and surrounding areas (asterisk). **D.** AQP4 immunoreactivity is extensively lost in not only the demyelinating center but also in the surrounding areas, where GFAP immunoreactivity is preserved (asterisk). **E.** High magnification of the area indicated by an arrowhead in C and D. Vascular foot processes are destroyed but there are remaining GFAP-positive astrocytes. **F.** The same microscopic field as in **E.** Astrocytes are devoid of AQP4 immunoreactivity. (**G–L**) Serial sections of chronic active Baló-like concentric lesions in the spinal cord from MS-4 representing Pattern A. **G.** The spinal cord shows concentric bands of alternating demyelination and preserved myelin. **H.** CD68-positive macrophages are still abundant in the lesions. **I.** GFAP immunostaining indicates strong gliosis at the lesion edge and surrounding areas. **J.** AQP4 immunoreactivity is completely lost in the lesion center and the surrounding area with preserved myelin staining (note the AQP4-immunopositive area only at the periphery of the spinal cord). **K.** High magnification of the blood vessels indicated by the arrowhead in **I** and **J** shows numerous GFAP-positive reactive astrocytes and remnant astrocytic vascular foot processes. **L.** In the same area as **K**, AQP4 immunoreactivity is completely lost in the GFAP-positive structures. **A, G**, KB; **B, H**, CD68 immunohistochemistry (IHC); **C, E, I, K**, GFAP IHC; **D, F, J, L**, AQP4 IHC. Scale bar = 500 μm (**G–J**); 300 μm (**A–D**); 50 μm (**E, F**); 30 μm (**K, L**). AQP4 = aquaporin-4; GFAP = glial fibrillary acidic protein; KB = Klüver-Barrera staining; MS = multiple sclerosis.

demyelinating lesions, GFAP immunostaining revealed highly degenerated astrocytic vascular foot processes (Figure 1E), and AQP4 expression was totally lost in these GFAP-immunopositive structures (Figure 1F).

In addition to the actively demyelinating lesions and necrotic lesions (Figure 1G, dagger, Figure 1K), still-myelinated areas at the lesion periphery occasionally showed a remarkable decrease in both GFAP and AQP4 expression in Pattern A, which was considered to represent early lesions (Figure 1G–O, asterisk in G). In such lesions, GFAP immunostaining revealed remaining highly degenerated astrocytes and their vascular foot processes (Figure 1N). Despite the existence of remnant astrocytes, AQP4 immunoreactivity was hardly detectable in such lesions (Figure 1O).

In contrast to the loss of both GFAP and AQP4 expression in acute lesions in this group, all the chronic inactive lesions in the NMO/NMOSD cases, including those in the anti-AQP4 antibody-seropositive case (NMO-10; Figure 2A–D), showed upregulation of AQP4 in areas with various degrees of reparative gliosis (either Pattern C or D) (Figure 2, Table 4).

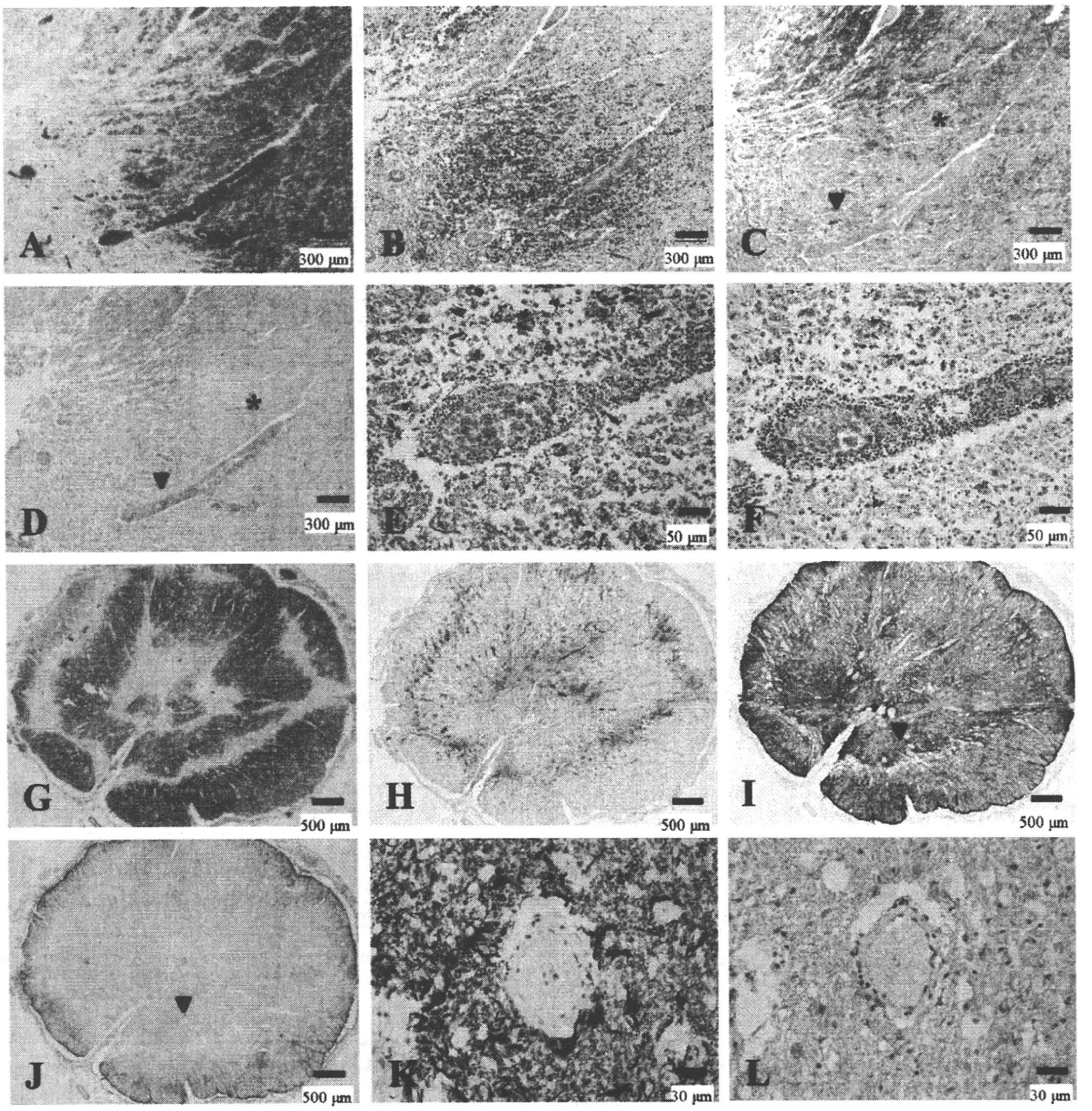

Figure 5. Distinctive patterns of perivascular immunoglobulin/complement deposition and lymphocytic cuffing between NMO and MS. (**A–D**) Active lesions in NMO with immunoglobulin/complement deposition. (**A, B**) Serial sections of a periplaque, still-myelinated area of NMO-4. These figures show the same area as that indicated by the arrowhead in Figure 1, G and I. IgM (**A**) and C3d (**B**) deposition are observed in astrocytic vascular foot processes as well as in degenerated astrocytes (arrowheads). (**C, D**) Serial sections from a more advanced active lesion in the spinal cord from NMO-7. IgG (**C**) and IgM (**D**) deposition are observed in astrocytic vascular foot processes as well as degenerated astrocytes (arrowheads). (**E–H**) Serial sections of an active lesion from NMO-10 without immunoglobulin/complement deposition. These figures show the periplaque, still-myelinated areas of the lesion shown in Figure 1A–F. Although GFAP immunoreactivity is preserved (**E**), AQP4 expression is totally lost (**F**). Neither C9neo (**G**) nor IgG (**H**) staining shows specific perivascular deposition. (**I, J**) Lack of immunoglobulin/complement deposition in MS. Serial sections of a chronic active lesion from MS-4. These figures show the same area as in Figure 4K and L. Neither IgG (**I**) nor C3d (**J**) staining shows typical perivascular deposition. (**K–M**) Lymphocyte cuffing in MS and NMO. (**K, L**) Serial sections from an active lesion from MS-3. These figures show the same lesion as in Figure 4E and F. **K.** CD45RO staining demonstrates perivascular cuffing predominantly consisting of T cells. **L.** Few CD20-positive B cells in the perivascular area. **M.** An active lesion in the spinal cord from NMO-7. This figure shows the same lesion as in **C** and **D**. Although CD45RO-positive T-cells predominate, the degree of perivascular lymphocyitic accumulation is much milder in NMO than in MS. **A, D**, IgM immunohistochemistry (IHC); **B, J**, C3d IHC; **C, H, I**, IgG IHC; **G**, C9neo IHC; **E**, GFAP IHC; **F**, AQP4 IHC; **K, M**, CD45RO IHC, **L**, CD20 IHC. Scale bar = 100 μm (**K, L**); 50 μm (**A–J, M**). AQP4 = aquaporin-4; GFAP = glial fibrillary acidic protein; KB = Klüver-Barrera staining; MS = multiple sclerosis; NMO = neuromyelitis optica.

Preserved AQP4 expression in actively demyelinating lesions in NMO cases

While the above-mentioned cases showed typical AQP4 and GFAP loss in active demyelinating lesions as reported previously (38, 45), five cases (NMO-1, 5, 6, 8 and 9) showed no preferential loss of AQP4 (Pattern D) in any lesions, including actively demyelinating lesions except for necrotic or cavitary lesions where no astrocytes were present (Pattern N) (Figure 3D–F, Table 4).

Heterogeneous AQP4 expression in actively demyelinating lesions

Among the NMO cases with preferential loss of AQP4 (Pattern A or B) in active lesions, we found a subset of cases showing lesion-to-lesion heterogeneity in AQP4 expression pattern, even among the active lesions (Figure 3G–L; compare with Figure 1G–O, Table 4). These included three NMO cases (NMO-4, 7 and 10) and one NMOSD case. Pattern D was observed in an active lesion in one case (NMO-4), and Pattern C was observed in chronic active lesions in five cases (NMO-2, 3, 4, 7 and 10) (Table 4). The NMO-4 case had repeated attacks of transverse myelitis and acutely developed a single episode of bilateral optic neuritis 1 month prior to death. As described earlier, the corpus callosum contained partially necrotized actively demyelinating lesions, with diminished AQP4 immunoreactivity extending over the loss of myelin staining and areas with reactive astrocytes, representing Patterns A and N (Figure 1G–O). Approximately half of the actively demyelinating lesions in this case were classified as Pattern A (Table 4). By contrast, the optic chiasm had actively demyelinating lesions densely infiltrated with macrophages containing myelin debris (Figure 3G–I), where both GFAP and AQP4 was expressed diffusely in the demyelinated lesions and the surrounding normal-looking areas (Figure 3J, K). At higher magnification, the demyelinating lesions were diffusely stained for AQP4 (Figure 3L) in many hypertrophic astrocytes and their processes, being classified as Pattern D.

Immunohistochemical findings in MS

Three MS cases (MS-1, 2 and 5) showed preservation of AQP4 in actively demyelinating lesions, whereas the other two (MS-3 and 4) showed preferential AQP4 loss in active lesions of both acute and chronic stages (Pattern A or B) (Table 5). All the MS cases showed AQP4 immunoreactivity in gliotic areas of chronic inactive lesions, if present (Pattern C or D) (Table 5).

Preferential decrease of AQP4 staining in actively demyelinating lesions

The MS-3 case had cerebral signs at disease onset and brainstem signs at relapse, but neither optic neuritis nor myelitis was noted. Notably, AQP4 loss was observed in both the centers of actively demyelinating plaques with dense perivascular lymphocytic cuffing in the cerebral peduncle, and in the periphery of the lesions where KB staining indicated preserved myelin with diffuse macrophage infiltration. This lesion was thus classified as Pattern A (see asterisks in Figure 4A–D). At higher magnification, GFAP immunostaining revealed degeneration of astrocytes and disruption of the perivascular glia limitants (Figure 4E). AQP4 expression was almost totally lost even in the scattered GFAP-positive structures (Figure 4F).

Loss of AQP4 expression in BCS-like concentric spinal cord lesions in an MS case

MS-4 had concentric lesions showing alternating rings with and without myelin in the chronic active stage, accompanied by perivascular macrophage infiltration in the spinal cord (Figure 4G, H). AQP4 loss was seen not only in the sharply demyelinated layers but also in the preserved myelin layers, and this lesion was classified as Pattern A (Figure 4I, J). High magnification demonstrated that AQP4 expression was lost on the astrocytic processes and reactive astrocytes, even though they were positive for GFAP (Figure 4K, L).

The actively demyelinating lesions in these two cases were classified as Pattern A or B (loss of AQP4).

Relationship between complement and immunoglobulin deposition and AQP4 loss

In the actively demyelinating lesions of the NMO/NMOSD cases, depositions of activated complement and immunoglobulins in the

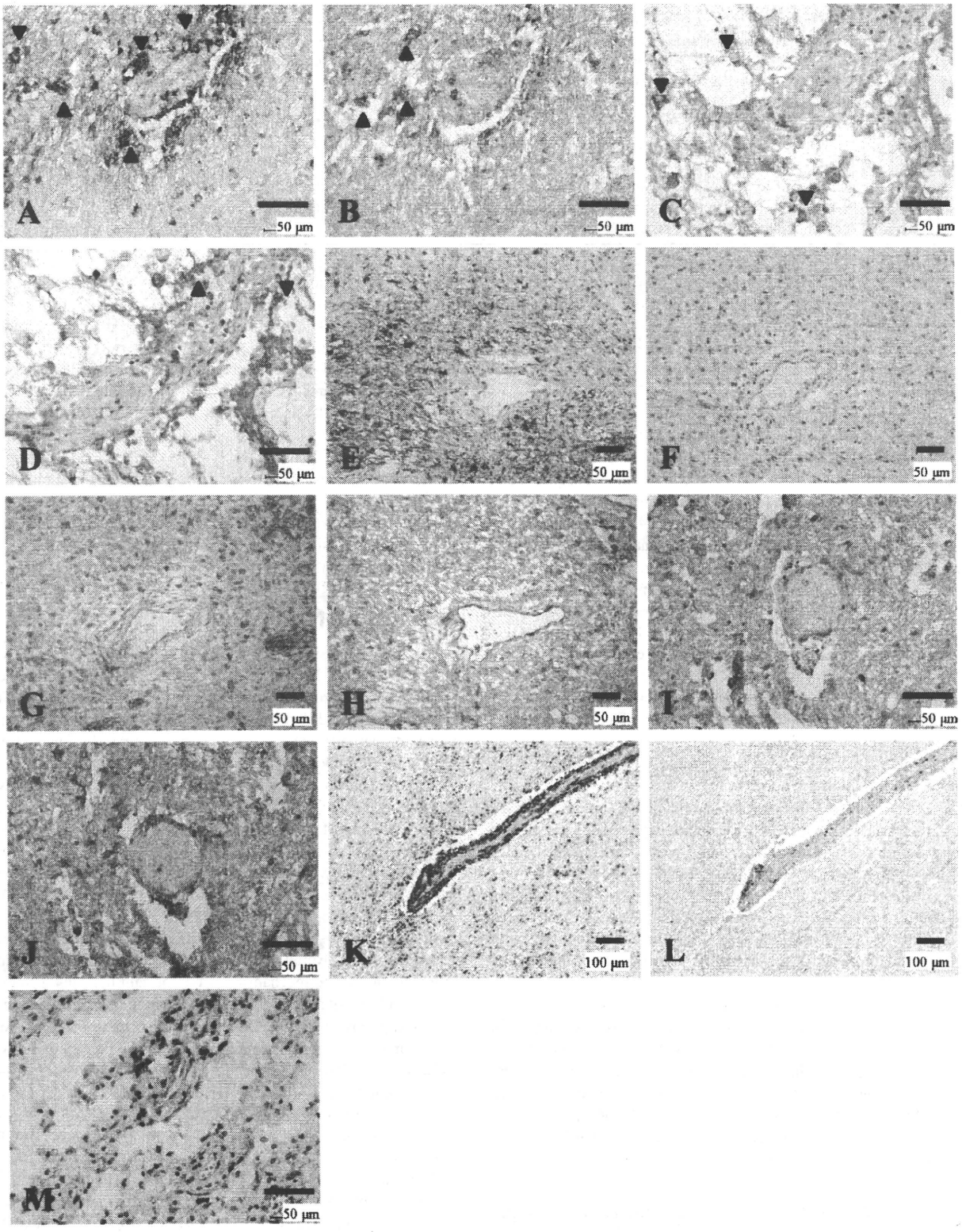

Figure 6. Heterogeneity between perivascular deposition of activated complement and immunoglobulins and AQP4 expression. (**A–G**) Serial sections of the peripheral area of chronic active lesions in the cerebral white matter of NMO-10. **A.** Demyelinating lesions confined to the vicinity of blood vessels. **B.** No inflammatory cell infiltration. **C.** AQP4 immunoreactivity on astrocyte processes. Immunoreactivities to activated complement (C3d (**D**) and C9neo (**E**)) and immunoglobulins (IgM (**F**) and IgG (**G**)) in the perivascular areas. Note that one blood vessel does not show deposition of activated complement or immunoglobulins (arrow in **D–G**). (**H–L**) Serial sections in the cerebral white matter of the same case. **H.** A chronic inactive demyelinating lesion. **I.** Few CD68-positive macrophages in the lesion. **J.** AQP4 labeling of the astrogliosis covering the lesions. C3d (**K**) and IgG (**L**) immunoreactivities are most intense in the perivascular area. (**M–O**) Serial sections of a chronic active demyelinating lesion in the spinal cord of the same case. **M.** Loss of AQP4 immunoreactivity is confined to the perivascular areas associated with C3d (**N**) and IgM (**O**) deposition. **A, H**, KB; **B, I**, CD68 immunohistochemistry (IHC); **C, J, M**, AQP4 IHC; **D, K, N**, C3d IHC; **E**, C9neo IHC; **F, O**, IgM IHC; **G, L**, IgG IHC. Scale bar = 100 μm (**A–G**); 50 μm (**H–O**); 15 μm (**C**). AQP4 = aquaporin-4; GFAP = glial fibrillary acidic protein; KB = Klüver-Barrera staining; NMO = neuromyelitis optica.

perivascular areas were observed in 28.6% of Pattern A lesions (Figures 5A–H and 7A). In chronic active lesions, such depositions were noted in 10%–15% of Patterns A, B and C. In chronic inactive lesions, one of 17 (6%) Pattern D lesions had perivascular deposits. However, MS cases did not have depositions in any demyelinated lesion (Figure 5I, J).

Four of the six cases with NMO/NMOSD that had AQP4 loss (Pattern A) showed concurrent perivascular deposition of activated complement and immunoglobulins in at least one actively demyelinating lesion. This represented 36% (4/11) of all NMO/NMOSD cases (Figure 7C). All of these cases demonstrated heterogeneity in the relationship between AQP4 loss and perivascular deposition of activated complement and immunoglobulins. Moreover, we also observed different patterns of AQP4 loss and perivascular deposition of activated complement and immunoglobulins even within a single lesion. For example, in NMO-10 with anti-AQP4 antibody, in the active cerebral lesions where AQP4 was totally lost, there was no deposition of either immunoglobulin or complement (Figure 5E–H). On the other hand, in the peripheral area of a chronic active demyelinating lesion (Pattern C) in the cerebral white matter, there were blood vessels surrounded by myelin showing variable degrees of diminished staining (Figure 6A). There was no macrophage infiltration or decreased AQP4 immunoreactivity in this area (Figure 6B, C), despite deposition of activated complement and immunoglobulins around some blood vessels (Figure 6D–G). Another chronic inactive lesion in the cerebral white matter, where AQP4 immunoreactivity was markedly increased (Figure 6H–J), showed perivascular deposits of activated complement and immunoglobulins (Figure 6K, L). However, chronic active lesions in the spinal cord demonstrated loss of AQP4 immunoreactivity with perivascular staining for complement and immunoglobulins (Figure 6M–O).

Areas with complement and immunoglobulin deposition, but without either demyelination or AQP4 loss (as shown in Figure 6B–G), were noted in five cases (three of the four NMO/NMOSD cases that showed concurrent perivascular complement and immunoglobulin deposition and AQP4 loss in some lesions, and one NMO/NMOSD case and one MS case that showed perivascular complement and immunoglobulin deposition, but neither AQP4 loss nor demyelination).

Relationship between perivascular lymphocytic cuffing and AQP4 loss

The frequency of each AQP4 expression pattern is summarized in Table 6. In actively demyelinating lesions, 23 of 38 (60.5%) Pattern A or B lesions (51.9% in NMO/NMOSD and 81.8% in MS) and eight of 16 (50.0%) Pattern D lesions (55.6% in NMO/NMOSD, and 42.9% in MS) showed perivascular lymphocytic cuffing. In total, perivascular cuffing was observed in 60% of the actively demyelinating lesions, regardless of clinical phenotype or AQP4 status (Figures 5K–M and 7B). In chronic active lesions, seven of 32 (21.9%) Pattern A or B lesions (16.0% in NMO/NMOSD and 42.9% in MS) and six of 42 (14.3%) Pattern D lesions (13.9% in NMO/NMOSD and 16.7% in MS) demonstrated perivascular lymphocytic cuffing. Generally, lymphocytic cuffing was milder in NMO/NMOSD than in MS. In addition, all lesions had predominant T-cell infiltration (30 in actively demyelinating lesions and 12 in chronic active lesions) (see Figure 5K–M).

DISCUSSION

We performed a systematic immunohistopathological study on autopsied cases of NMO and MS. Half of NMO patients showed preferential loss of AQP4 beyond the area of demyelination, whereas others did not, even in actively demyelinating lesions. Some MS patients, including one with only brain lesions and the other with BCS-like concentric spinal cord lesions, demonstrated extensive AQP4 loss in actively demyelinating and chronic active lesions, whereas other MS patients showed preservation of AQP4. Even NMO and MS patients with preferential AQP4 loss showed AQP4 patterns that varied from lesion to lesion, with no AQP4 loss in some of the actively demyelinating lesions, as well as in chronic active and inactive lesions. Vasculocentric deposition of complement and immunoglobulins was specifically noted in a third of NMO/NMOSD cases, but did not tightly correlate with perivascular AQP4 loss. Overall, our study indicates that antibody and complement-related mechanisms are important in AQP4 astrocytopathy in a fraction of NMO cases, as seen in one case with anti-AQP4 antibody, but AQP4 loss can also occur in some actively demyelinating MS lesions, and can occasionally be very extensive, as seen in the Baló-like concentric spinal cord lesions of MS-4. Furthermore, the lesion-to-lesion heterogeneity in the AQP4 expression pattern observed in NMO cases implies a heterogeneous relationship between anti-AQP4 antibody and loss of AQP4 expression.

Our study has some limitations inherent to studies using archival autopsied materials. First, because the autopsied cases died with the disease, there was a potential bias toward severe cases. Our histological evaluation focusing on early active lesions and separately analyzing necrotic lesions can minimize this selection bias. Second, the anti-AQP4 antibody status was only known in one case,

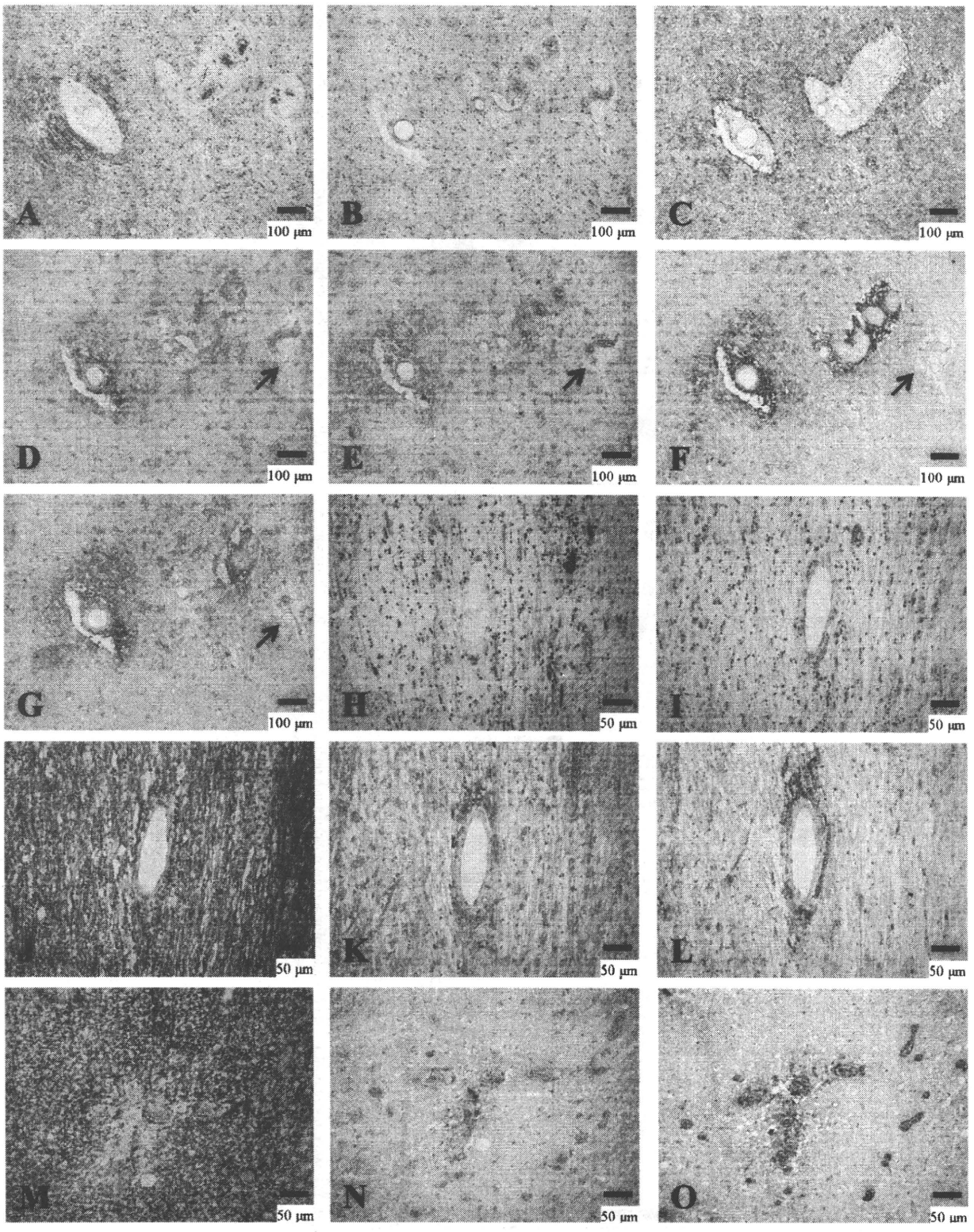

Figure 7. A. Positive rates of perivascular complement and immunoglobulin deposition in NMO/NMOSD cases according to AQP4 patterns and lesion stage. Because no MS case showed such depositions, only NMO/NMOSD lesions are included here. n = the number of demyelinating lesions. **B.** Positive rates of perivascular lymphocytic cuffing in the actively demyelinating and chronic active lesions according to AQP4 patterns and clinical phenotypes. n = the number of demyelinating lesions; see Table 3 for the definitions of the patterns. Any pattern with necrosis (Patterns X & N) was included in Pattern X. **C.** The relationship between AQP4 expression patterns and immunoglobulin/complement deposition in each disease type. The data on Baló's disease is cited from our previous report (33). AQP4 = aquaporin-4; MS = multiple sclerosis; NMO = neuromyelitis optica; NMOSD = NMO spectrum disorder.

Table 6-1. Frequency of each aquaporin-4 immunoreactivity pattern in demyelinating lesions from cases with neuromyelitis optica (NMO) or NMO spectrum disorders. Abbreviations: NMO = neuromyelitis optica; NMOSD = neuromyelitis optica spectrum disorder.

Lesion pattern	NMO and NMOSD (n = 149)		
	Active (n = 42)	Chronic active (n = 72)	Chronic inactive (n = 35)
Pattern A	17	13	0
Pattern B	10	12	0
Pattern C	0	11	9
Pattern D	9	36	23
Pattern N	6	0	3

Table 6-2. Frequency of each aquaporin-4 immunoreactivity pattern in demyelinating lesions from cases with multiple sclerosis. Abbreviations: MS = multiple sclerosis.

Lesion pattern	MS (n = 51)		
	Active (n = 24)	Chronic active (n = 14)	Chronic inactive (n = 13)
Pattern A	4	4	0
Pattern B	7	3	0
Pattern C	0	1	1
Pattern D	7	6	12
Pattern N	6	0	0

See Table 3 for the definition of the patterns. Any pattern with necrosis (Patterns X and N) was included into Pattern X.

because the other autopsies were performed before the discovery of NMO-IgG. These limitations are common to the other pathological studies on AQP4 expression in NMO by Misu *et al* (38) and Roemer *et al* (45). We were able to evaluate AQP4 expression in the one NMO case with confirmed anti-AQP4 antibodies, which enabled a detailed evaluation of the relationship between the presence of anti-AQP4 antibody and AQP4 expression in the CNS.

The results of our study are somewhat discordant with those of previous studies (38, 45), which might, in part, be attributable to the differences in methodology and materials. Regarding the staining method, in our previous (33) and present studies, we found AQP4 expression patterns similar to those reported in normal and diseased control brain tissues (1, 27, 38, 45) despite using a different anti-AQP4 antibody. The evaluation of necrotic lesions also requires some consideration. In necrotic lesions totally replaced by macrophages where no viable astrocytes existed, we could not differentiate whether the loss of AQP4 was caused by down-modulation of AQP4 in astrocytes or the loss of astrocytes *per se*. Furthermore, in such destructive lesions, it would be difficult to determine the causal relationship between AQP4 loss and the astrocyte damage. Therefore, we decided to put more stress on evaluating earlier lesions where the background tissues were still relatively preserved. Although the clinical features of MS are somewhat different between northern (Misu's cases) and southern Japanese (our cases) (15, 41), these differences in methodology should not seriously distort our results.

Half of our NMO cases showed a preferential loss of AQP4 in actively demyelinating and chronic active lesions, whereas the rest did not, despite severe tissue destruction. This is in line with the fact that anti-AQP4 antibody is not detected in 30%–70% of NMO cases (22). Vasculocentric complement and immunoglobulin deposition was noted only in NMO/NMOSD cases but not in MS cases. These findings support the notion that AQP4 loss in NMO cases results from immune responses to AQP4 (38, 45). Accordingly, it is possible that pathologically, there are two types of NMO, namely AQP4 autoimmunity-related and AQP4 autoimmunity-unrelated, and the latter may correspond clinically to seronegative NMO (31, 35).

The vasculocentric deposition of complement and immunoglobulins was only detected in NMO patients with AQP4 loss, including one with anti-AQP4 antibody. This supports the hypothesis that anti-AQP4 antibody destroys perivascular astrocyte foot processes via complement-dependent mechanisms. However, more than half of the AQP4-down-modulated NMO lesions showed no vasculocentric deposition of complement and immunoglobulins. This might be caused by very transient complement and immunoglobulin deposition. We staged NMO lesions with myelin-laden macrophages as active according to the lesion staging in MS; however, it is possible that complement/immunoglobulin deposition rapidly disappears even in the presence of myelin-laden macrophages once it triggers the astrocytic damage. Alternatively, the findings might be interpreted, such that the anti-AQP4 antibody and complement-mediated mechanism is unique to NMO, but does not always accompany every lesion. Further studies are necessary to clarify the time course of complement/immunoglobulin deposition during the formation of NMO lesions in an experimental model.

Our pathological study also argues against autoimmune AQP4 destruction as the sole NMO mechanism. First, the severity of tissue destruction was unrelated to tissue AQP4 loss or preservation. Second, AQP4 expression was heterogeneous even in the same individual. Although chronic inactive lesions may restore AQP4 expression with astrogliosis, one NMO case showed preservation of AQP4 in actively demyelinating optic chiasmal lesions, despite reduced AQP4 expression in other CNS lesions. Third, the perivascular deposition of complement and immunoglobulins did not closely correlate with perivascular AQP4 loss.

Anti-AQP4 antibody titer could change from patient to patient and between different disease stages in the same patient, which might have affected AQP4 expression levels in the pathological lesions. However, in this case, the existence of actively demyelinating lesions without AQP4 loss in NMO patients showing preferential AQP4 loss in other active lesions suggests that anti-AQP4 antibody does not always play a primary role in initiating inflammatory lesions. Other factor(s) may be responsible for triggering the pathological features, which are then modulated by anti-AQP4 antibodies. To clarify the real consequences of this autoantibody, a prospective neuropathological study based on anti-AQP4 antibody status is required.

Regarding MS, somewhat inconsistent results have been reported. Misu *et al* (38) reported no loss of AQP4 in MS plaques, whereas Roemer *et al* (45) found stage-dependent loss of AQP4, with inactive MS lesions showing complete AQP4 loss. On the other hand, Sharma *et al* (48) observed patchy AQP4 loss only in a subset of active lesions following pattern III MS lesions. These authors found loss of perivascular astrocytic foot processes where AQP4 was lost, while numerous reactive astrocytes had intense AQP4 immunoreactivity in the lesions. In our study, AQP4 expression was decreased or totally lost in acute and chronic active

demyelinating lesions in a fraction of MS cases, including one that lacked optic nerve and spinal cord lesions. At the cellular level, disruption of astrocytic vascular foot processes was evident in such lesions, and AQP4 expression was lost in both cell bodies and vascular foot processes of astrocytes as seen in acute NMO lesions. Our present and previous findings (33) raise the possibility that AQP4 loss *per se* is not confined to NMO, but rather, that it could also occur in actively demyelinating lesions of MS and BCS, suggesting a notion that astrocyte damage accompanied by AQP4 loss is not always related to anti-AQP4 antibody. Sharma *et al* (48) also reported that autoantibody-independent AQP4 loss and astrocytic dysfunction occurs in lipopolysaccharide-induced experimental demyelination, providing experimental support for such a notion. Interestingly, Baló-like concentric lesions in the spinal cord of MS-4 also showed similar extensive AQP4 loss to BCS, including in the areas of preserved myelin. We previously found no vasculocentric deposition of complement and immunoglobulin in BCS cases (33), and we and others (2) also demonstrated no such perivascular deposition in MS. Thus, extensive AQP4 loss without perivascular deposition of complement and immunoglobulin may be a common pathological feature of at least a subset of the concentric lesions in BCS and MS.

In summary, antibody-mediated AQP4 astrocytopathy occurs only in NMO, whereas antibody-independent AQP4 astrocytopathy can develop in various demyelinating conditions, including MS, BCS and a fraction of NMO cases (Figure 7C). Further studies on astrocytopathy as well as the dynamic plasticity of astrocytes in demyelinating diseases may shed light on the mechanisms underlying MS and allied disorders.

ACKNOWLEDGMENTS

This work was supported in part by grants from the Research Committees of Neuroimmunological Diseases, the Ministry of Health, Labor and Welfare, Japan, and from the Ministry of Education, Culture, Sports, Science and Technology, Japan. We thank Sachiko Nagae and Kimiko Sato, Department of Neuropathology, Kyushu University, for their excellent technical assistance, and Takekazu Ohi, Department of Neurology, Kurashiki Central Hospital, for providing materials.

REFERENCES

1. Aoki K, Uchihara T, Tsuchiya K, Nakamura A, Ikeda K, Wakayama Y (2003) Enhanced expression of aquaporin 4 in human brain with infarction. *Acta Neuropathol* **106**:121–124.
2. Barnett MH, Parratt JD, Cho ES, Prineas JW (2009) Immunoglobulins and complement in postmortem multiple sclerosis tissue. *Ann Neurol* **65**:32–46.
3. Bennett JL, Lam C, Kalluri SR, Saikali P, Bautista K, Dupree C *et al* (2009) Intrathecal pathogenic anti-aquaporin-4 antibodies in early neuromyelitis optica. *Ann Neurol* **66**:617–629.
4. Bot JC, Barkhof F, Polman CH, Lycklama a Nijeholt GJ, de Groot V, Bergers E *et al* (2004) Spinal cord abnormalities in recently diagnosed MS patients: added value of spinal MRI examination. *Neurology* **62**:226–233.
5. Bradl M, Misu T, Takahashi T, Watanabe M, Mader S, Reindl M *et al* (2009) Neuromyelitis optica: pathogenicity of patient immunoglobulin *in vivo*. *Ann Neurol* **66**:630–643.
6. Cabrera-Gomez JA, Bonnan M, Gonzalez-Quevedo A, Saiz-Hinarejos A, Marignier R, Olindo S *et al* (2009) Neuromyelitis optica positive antibodies confer a worse course in relapsing-neuromyelitis optica in Cuba and French West Indies. *Mult Scler* **15**:828–833.
7. Chen CJ, Chu NS, Lu CS, Sung CY (1999) Serial magnetic resonance imaging in patients with Balo's concentric sclerosis: natural history of lesion development. *Ann Neurol* **46**:651–656.
8. Chong HT, Ramli N, Lee KH, Kim BJ, Ursekar M, Dayananda K *et al* (2006) Magnetic resonance imaging of Asians with multiple sclerosis was similar to that of the West. *Can J Neurol Sci* **33**:95–100.
9. Collongues N, Marignier R, Zephir H, Papeix C, Blanc F, Ritleng C *et al* (2010) Neuromyelitis optica in France: a multicenter study of 125 patients. *Neurology* **74**:736–742.
10. Fazio R, Malosio ML, Lampasona V, De Feo D, Privitera D, Marnetto F *et al* (2009) Antiacquaporin 4 antibodies detection by different techniques in neuromyelitis optica patients. *Mult Scler* **15**:1153–1163.
11. Graber JJ, Kister I, Geyer H, Khaund M, Herbert J (2009) Neuromyelitis optica and concentric rings of Balo in the brainstem. *Arch Neurol* **66**:274–275.
12. Hung TP, Landsborough D, Hsi MS (1976) Multiple sclerosis amongst Chinese in Taiwan. *J Neurol Sci* **27**:459–484.
13. Ikota H, Iwasaki A, Kawarai M, Nakazato Y (2010) Neuromyelitis optica with intraspinal expansion of Schwann cell remyelination. *Neuropathology* **30**:427–433.
14. Ikuta F, Koga M, Takeda S, Ohama E, Takeshita I, Ogawa H (1982) Comparison of MS pathology between 70 American and 75 Japanese autopsy cases. In: *Multiple Sclerosis East and West*, Y Kuroiwa, LT Kurland (eds), pp. 297–306. Kyushu University Press: Fukuoka.
15. Ishizu T, Kira J, Osoegawa M, Fukazawa T, Kikuchi S, Fujihara K *et al* (2009) Heterogeneity and continuum of multiple sclerosis phenotypes in Japanese according to the results of the fourth nationwide survey. *J Neurol Sci* **280**:22–28.
16. Itoyama Y, Tateishi J, Kuroiwa Y (1985) Atypical multiple sclerosis with concentric or lamellar demyelinated lesions: two Japanese patients studied post mortem. *Ann Neurol* **17**:481–487.
17. Jarius S, Franciotta D, Bergamaschi R, Wright H, Littleton E, Palace J *et al* (2007) NMO-IgG in the diagnosis of neuromyelitis optica. *Neurology* **68**:1076–1077.
18. Jung JS, Bhat RV, Preston GM, Guggino WB, Baraban JM, Agre P (1994) Molecular characterization of an aquaporin cDNA from brain: candidate osmoreceptor and regulator of water balance. *Proc Natl Acad Sci U S A* **91**:13052–13056.
19. Kinoshita M, Nakatsuji Y, Kimura T, Moriya M, Takata K, Okuno T *et al* (2009) Neuromyelitis optica: passive transfer to rats by human immunoglobulin. *Biochem Biophys Res Commun* **386**:623–627.
20. Kinoshita M, Nakatsuji Y, Moriya M, Okuno T, Kumanogoh A, Nakano M *et al* (2009) Astrocytic necrosis is induced by anti-aquaporin-4 antibody-positive serum. *Neuroreport* **20**:508–512.
21. Kinoshita M, Nakatsuji Y, Kimura T, Moriya M, Takata K, Okuno T *et al* (2010) Anti-aquaporin-4 antibody induces astrocytic cytotoxicity in the absence of CNS antigen-specific T cells. *Biochem Biophys Res Commun* **394**:205–210.
22. Kira J (2010) Neuromyelitis optica and opticospinal multiple sclerosis: mechanisms and pathogenesis. *Pathophysiology* **18**:69–79.
23. Kishimoto R, Yabe I, Niino M, Sato K, Tsuji S, Kikuchi S, Sasaki H (2008) Balo's concentric sclerosislike lesion in the brainstem of a multiple sclerosis patient. *J Neurol* **255**:760–761.
24. Kobayashi Z, Tsuchiya K, Uchihara T, Nakamura A, Haga C, Yokota O *et al* (2009) Intractable hiccup caused by medulla oblongata lesions: a study of an autopsy patient with possible neuromyelitis optica. *J Neurol Sci* **285**:241–245.